Progress In Electromagnetics Research C, Vol. 118, 71–81, 2022

Compact Ultrawideband Monopole Antenna with Continuously Tunable Notch Band Characteristics

Nooshin Moradi[1], Farid Nazari[2], Hadi Aliakbarian[2], and Farhad Azadi Namin[1, *]

Abstract—In this work, a planar monopole ultrawideband (UWB) antenna with continuously tunable notch band feature is presented. The designed antenna, which has a compact size of $36.6 \times 26 \times 1\,\text{mm}^3$, is fabricated on a low-cost FR4 substrate and comprises a circular radiating patch with four rectangular defects, a microstrip feed line, and a partial ground plane to cover the UWB frequency band extending from 3.1 GHz to 12.5 GHz. A semi-elliptical slot is etched out from the circular patch to create the first notch band at 3.6 GHz (WiMAX) in the UWB spectrum. The second notch band is created by embedding an annular slot on the circular patch loaded with a varactor diode to continuously tune the notch frequency from 5.6 GHz to 7.7 GHz in upper WLAN and X-band. To investigate the implementation feasibility of the designed UWB antenna, a prototype is fabricated and experimentally tested.

1. INTRODUCTION

Over the last few years, there has been an immense focus on UWB systems [1] in both telecommunications and radar applications due to their multiple advantages such as high data rate, low expenses, low power consumption, reduction of multipath fading, high accuracy, resolution, low system complexity, and wireless connectivity. Among the numerous antenna designs for UWB applications, compact planar monopole antennas are an ideal choice due to their simple structures, light weight construction, wide impedance bandwidth, and omnidirectional radiation pattern [2, 3].

In 2002, Federal Communication Commission (FCC) assigned the frequency range 3.1 to 10.6 GHz for UWB communication [4]. UWB antennas cover a wide range of the electromagnetic spectrum. However, many other narrowband services interfere with the UWB, such as the global interoperability for microwave access (WiMAX) 3.5 GHz, wireless local area network (WLAN) 5.2 GHz and 5.8 GHz, and X-band satellite communication systems 7.5 GHz.

UWB antennas with varied band-notch parameters are designed and built to eliminate UWB-narrowband interference [5–17]. Antennas for UWB are categorized into three types based on notch characteristics: 1) fixed band notch frequencies [5–10], 2) reconfigurable band notch frequencies [11, 12], and 3) continuously tunable notch bands [13–17]. A WLAN band notch is created by a sectorial-circular slot in the radiating patch [5]. To achieve two rectangular notch bands, a U-slot, two split-ring resonators, and two electromagnetic band gap (EBG) structures were added to the radiating patch and backside [6]. Two dual-band meander ground defects and negative permittivity unit cells formed quadruple notch bands in [7, 8]. In [9], five notch bands are achieved by etching several slots at five center notched frequencies. Six rejection bands between 2.96 and 8.06 GHz are achieved with two SRRs and four U-shaped parasitic strips [10]. Two PIN diodes employed in two double split ring resonators (DSRRs) produce two reconfigurable notch bands between WiMAX and HiperLAN2 [11]. Multiple PIN diodes switching between ON/OFF can achieve several notch band frequencies [12]. In [13], continuously

Received 2 December 2021, Accepted 21 January 2022, Scheduled 31 January 2022

* Corresponding author: Farhad Azadi Namin (namin_farhad@aut.ac.ir).

[1] Department of Electrical Engineering, Amirkabir University of Technology (Tehran Polytechnic), Tehran, Iran. [2] Department of Electrical Engineering, K. N. Toosi University of Technology, Tehran, Iran.

tunable band notch behavior between WLAN and WiMAX is achieved using two capacitors. Two varactor diodes in the structure provide dual tunable band notch frequencies below and above 5 GHz [14]. Both reconfigurable (bandpass/bandstop) and tunable behaviors are provided in [15], by loading the S-shaped SRRs with a pair of PIN diodes and a varactor diode. A UWB filtering monopole antenna with three continuously tunable rejection bands is introduced in [16]. Three varactor diodes placed between the SRR gaps allow for triple adjustable notch band frequencies which are achieved in [17].

Tunable structures have gained a lot of attention in wireless communications because they can prevent fabrication defects and can be tuned in real-time. That is why UWB antennas with continuously tunable notch performances over the UWB spectrum are of particular interest. In this paper, a dual notch band monopole antenna for UWB applications is designed and fabricated to show radiating characteristics in the frequency range 3.1–12.5 GHz. In Section 2, a semi-elliptical slot centered at 3.6 GHz and an annular slot centered at 7.4 GHz are embedded on the radiating patch to create two rejection bands. In order to achieve the tunability feature, a varactor diode with the junction capacitance ranging from 0.466 to 2.35 pF is loaded on the annular slot to tune the second notch band in the frequency range 5.6 GHz–7.7 GHz. In Section 3, the designed UWB antenna with a continuously tunable notch band is fabricated, and good agreement between simulated and measured results is achieved. A conclusion is rendered in Section 4. All of the numerical simulations obtained in this paper are carried out by CST Microwave Studio software [18].

2. DESIGN PROCEDURES

The designed dual notch band UWB antenna's schematic configuration and dimension specifications are displayed in Fig. 1 and Table 1, respectively. The designed antenna is fed by a 50 Ω microstrip line and designed on FR-4 substrate material with overall size $L_{sub} \times W_{sub}$, thickness $h = 1$ mm, dielectric constant $\varepsilon_r = 4.3$, and loss tangent $\tan\delta = 0.02$, which is placed on the partial ground plane. The design steps of the designed antenna beginning with the design of the UWB microstrip-fed monopole antenna and concluding with the final structure of the antenna producing notch bands are detailed as follows.

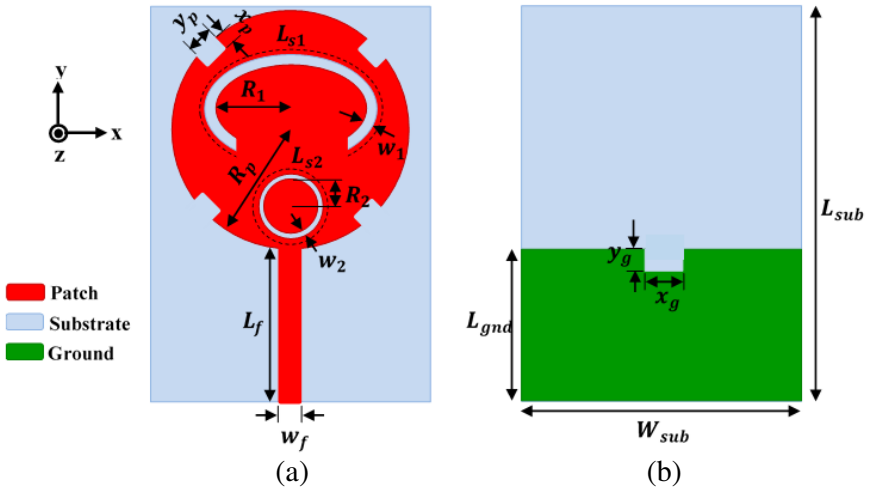

Figure 1. Configuration of the designed UWB antenna. (a) Top view and (b) bottom view.

2.1. Dual Notch Band UWB Antenna

The UWB monopole antenna consists of a circular radiating patch with the radius of R_p that is fed by a 50 Ω microstrip feed line with the length of L_f printed on the top of the FR-4 dielectric substrate, along with a partial ground plane with the length of L_{gnd} inserted on the bottom of the dielectric substrate. To improve impedance matching, the slot with dimensions of $x_g \times y_g$ and four rectangular defects with dimensions of $x_p \times y_p$ are etched out from ground plane and circular radiating patch, respectively. This

Table 1. Dimensions of the designed UWB antenna.

Parameter	Value (mm)	Parameter	Value (mm)
W_{sub}	26	R_2	2
L_{sub}	36.6	w_2	0.5
R_p	11	L_f	14.3
x_p	1	w_f	1.8
y_p	2	L_{gnd}	14
R_1	7	x_g	2.6
w_1	1	y_g	1.5

structure is considered as a reference UWB antenna with no band notch referred to as Ant. I and is shown in Fig. 2(a). The UWB frequency range is achieved from 3.1 GHz to 12.5 GHz as depicted in Fig. 3. Next, a dual notch band UWB antenna is achieved by etching out semi-elliptical and annular slots from the radiating patch. The length of the slot (L_s) at each notch frequency is approximately half of the guided wavelength (λ_g) and is calculated as follows [5]:

$$L_s = \frac{\lambda_g}{2} = \frac{\lambda_0}{2\sqrt{\varepsilon_{eff}}} = \frac{c}{2f_{\text{notch}}\sqrt{\varepsilon_{eff}}} \tag{1}$$

where λ_0, c, f_{notch}, and $\varepsilon_{eff} = (\varepsilon_r + 1)/2$ are the free space wavelength, speed of light, center frequency of the notch band, and effective dielectric constant, respectively.

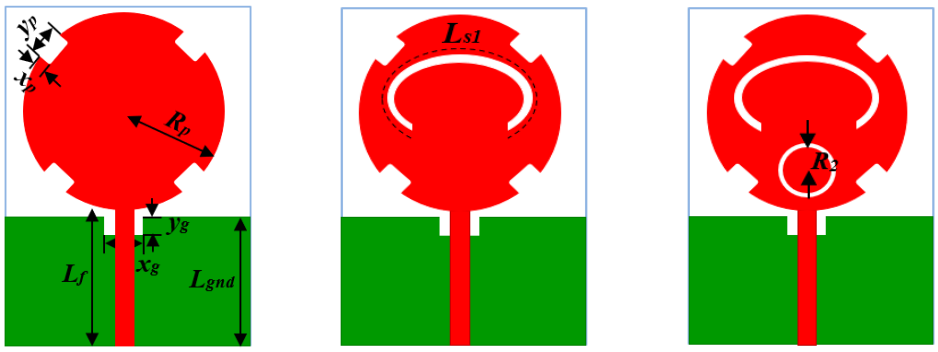

Figure 2. Schematics of (a) Ant. I, (b) Ant. II and (c) Ant. III.

The first notch band centered at $f_{\text{notch1}} = 3.6$ GHz is achieved by embedding a semi-elliptical shape slot in the radiating patch, whose length is $L_{s1} = 25.6$ mm using Eq. (1). It is referred to as Ant. II, and its schematic is shown in Fig. 2(b). In this way, the first notch band is obtained in 3.4–3.7 GHz, which will omit interference from the WiMAX band, as shown in Fig. 3. Full-wave simulation in the commercial software CST is used to optimize the position of this slot. Fig. 4(a) shows the simulation results of reflection coefficient (S_{11}) for various L_{s1} values. It is recognized that by controlling L_{s1}, the notch band can be adjusted. The center frequency of the notch band moves from a lower to a higher frequency as L_{s1} decreases, with no effect on UWB properties. As can be seen in Fig. 4(a), a notch band is formed centered at 3.3 GHz, 3.6 GHz, and 3.9 GHz corresponding to length L_{s1} of 28 mm, 25.6 mm, and 23.6 mm, respectively.

In a further study, an annular slot with $L_{s2} = 12.5$ mm is inserted on the radiating patch near the microstrip feed line, which we referred to as Ant. III as shown in Fig. 2(c), to produce a significant coupling between the patch and the finite ground plane. This slot generates the second notch band

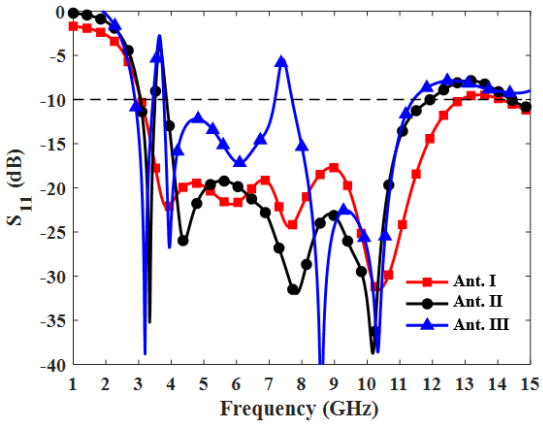

Figure 3. Simulated S_{11} versus frequency for antennas designed in Fig. 2.

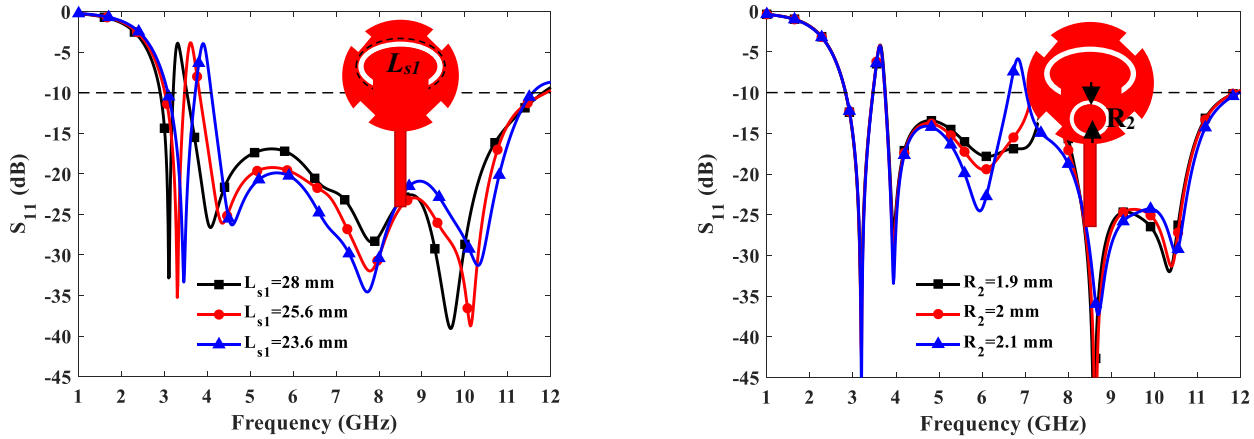

Figure 4. Simulated S_{11} versus frequency of the structure designed in Fig. 5 for different values of (a) the length of the semi-elliptical slot L_{s1} and (b) inner radius of the annular slot R_2.

centered at $f_{\text{notch2}} = 7.4\,\text{GHz}$, which can be noticed from Fig. 3. The center frequency of the second notch is specified by the annular slot's perimeter L_{s2} and can be changed by adjusting the radius of the annular slot $R_2 = L_{s2}/2\pi$, as illustrated in Fig. 4(b). It also seems to have a negligible effect on the first notch band. The frequency of the first notch is only dependent on the length of the semi-elliptical shape slot, namely L_{s1}. The second notch band is achieved at 7.7 GHz, 7.4 GHz, and 6.9 GHz, corresponding to radius R_2 of 1.9 mm ($L_{s2} = 12\,\text{mm}$), 2 mm ($L_{s2} = 12.5\,\text{mm}$), and 2.1 mm ($L_{s2} = 13.3\,\text{mm}$), respectively. Variations of slot widths have negligible effects on reflection coefficient, so for all parametric processes, they are set to $w_1 = 1\,\text{mm}$ and $w_2 = 0.5\,\text{mm}$.

2.2. Second Notch Band Tunability

In order to enable tunable notch band characteristics, a varactor diode is inserted in the gap inside the annular slot to tune the second notch band with the center frequency at 7.4 GHz for reducing electromagnetic interference with the WLAN (5.15–5.35 GHz, 5.725–5.825 GHz) and X-band (7.1–7.76 GHz) systems. The varactor diode SMV1231 was chosen in this structure [19]. The varactor diode's equivalent circuit model, which includes parasitic inductance ($L_p = 0.7\,\text{nH}$), series resistance ($R_s = 2.5\,\Omega$), parasitic capacitance ($C_p = 0.44\,\text{pF}$), and junction capacitance C_j, is shown in Fig. 5. The junction capacitance C_j provides variable capacitance from 0.466 pF to 2.35 pF (i.e., reverse bias voltage from 15 V to 0 V). The values of circuit parameters are listed in Table 2 [19].

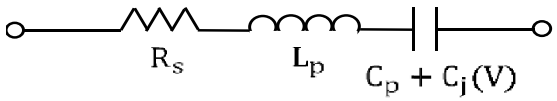

Figure 5. Equivalent circuit model of the varactor diode.

Table 2. The effective circuit parameters for the varactor diode used in the design [19].

V_R (V)	C_j (pF)	R_s (Ω)	L_p (nH)	C_p (pF)
0	2.35	2.5	0.7	0.44
1	1.58	2.5	0.7	0.44
2.5	1.09	2.5	0.7	0.44
5	0.683	2.5	0.7	0.44
10	0.497	2.5	0.7	0.44
15	0.466	2.5	0.7	0.44

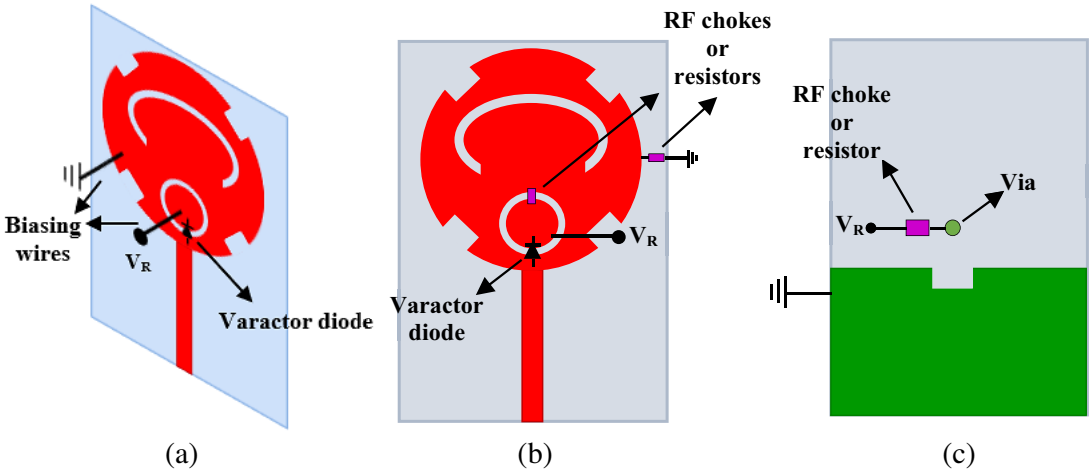

Figure 6. Schematics of various methods for applying reverse bias voltage V_R to the varactor diode: (a) method 1, (b) method 2, and (c) method 3.

The DC bias voltage route is required to be decoupled from the RF signal to avoid affecting high-frequency results. There are several ways to do this: 1) the wires connected to the varactor diode to apply reverse bias voltage should be as short as possible and placed perpendicular to the antenna surface. This method cannot be used in practical applications (Fig. 6(a)); 2) two RF chokes inductors or large resistors are loaded on the structure to confine the current passing by the varactor diode and block RF signals (Fig. 6(b)); and 3) to minimize the interaction between radiating patch and wires connected to DC source, RF choke or large resistor is located on the back of the structure using a via (Fig. 6(c)). In order to clarify the effectiveness of the proposed methods, the reflection coefficients (S_{11}) of the structures in Fig. 6 are compared with the state without biasing network for $C_j = 1.58\,\text{pF}$ ($V_R = 1\,\text{V}$) as shown in Fig. 7. In this paper, the second method is used to apply a reverse bias voltage to the varactor diode in the fabrication and measurement process. The simulated reflection coefficients (S_{11}) of the designed dual notch band UWB antenna for different values of the junction capacitance C_j are shown in Fig. 10(a). When the varactor diode operates at the smallest value of the junction capacitance, $C_j = 0.466\,\text{pF}$ (experimentally at the highest value of reverse bias voltage $V_R = 15\,\text{V}$), the second notch band is created at the center frequency of 7.7 GHz. When the junction capacitance increases to its

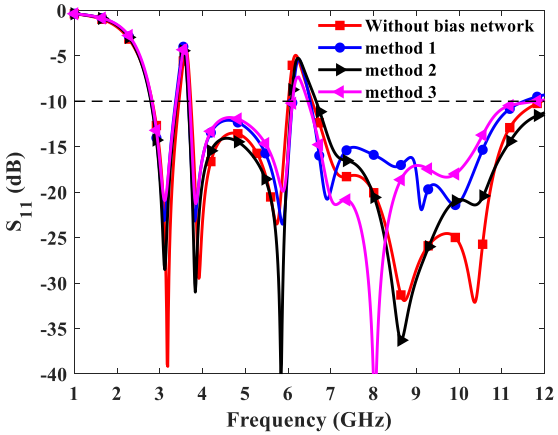

Figure 7. Simulated S_{11} versus frequency for the structures without and with biasing network in Fig. 6.

maximum value, $C_j = 2.35\,\text{pF}$ (experimentally the lowest value of the reverse bias voltage $V_R = 0\,\text{V}$), the second notch band occurs at 5.6 GHz. Therefore, by changing the junction capacitance, the second notch band frequency can be modified in a wide range from 5.6 GHz to 7.7 GHz, to prevent interference from systems operating in upper WLAN (5.725–5.825 GHz) and X-band (7.1–7.76 GHz).

To verify the band notch specifications, simulated surface current distribution for the designed dual notch band UWB antenna with junction capacitance $C_j = 1.58\,\text{pF}$ is shown in Fig. 8 for three frequencies: 3.4 GHz and 6.2 GHz, which are the first and second notch frequencies, and 8.7 GHz, which is an arbitrary operating frequency outside of the notch bands. At the first notch band centered at 3.6 GHz, as shown in Fig. 8(a), the current is concentrated around the semi-elliptical slot which leads to a high attenuation of radiation power at this frequency. As a result, the first notch is produced. It is obvious from Fig. 8(b) that at the second notch band centered at 6.2 GHz, the current mostly flows on the annular slot which satisfies the reason for this notch band. The current distribution is similar at other bias voltages. To express in more detail, currents around slots at notch frequencies distribute in opposite directions with the same values which counteract each other and cause no radiation at these frequencies. It is important to note that in Figs. 8(a)–(b), there is no mutual coupling at the notch frequencies; therefore, dual notch band UWB antenna is created. At the operating frequency 8.7 GHz, as shown in Fig. 8(c), the current flows on the entire patch surface, so that antenna radiates RF energy in passband.

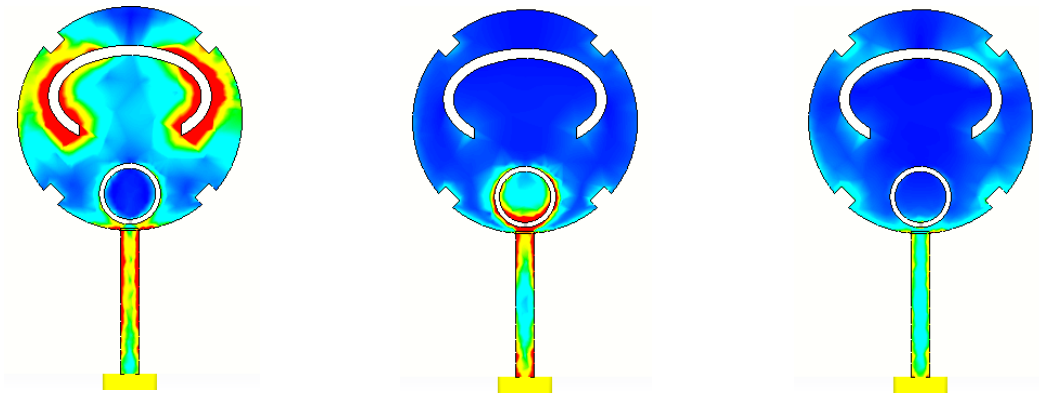

Figure 8. Current distribution of the designed dual notch band antenna with $C_j = 1.58\,\text{pF}$ at (a) 3.6 GHz, (b) 6.2 GHz, and (c) 8.7 GHz.

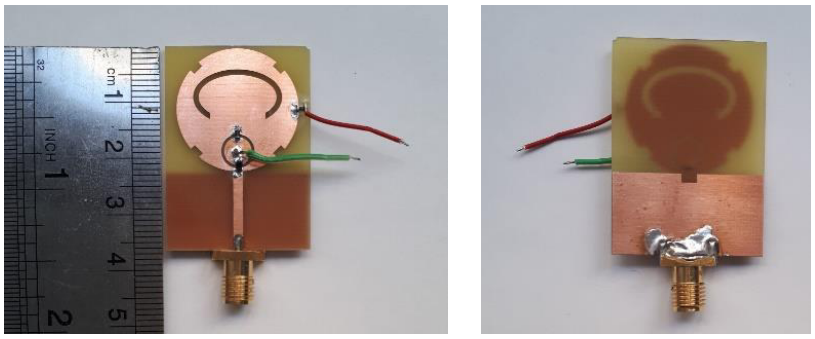

(a) (b)

Figure 9. Photographs of fabricated dual notch band UWB antenna: (a) top view and (b) bottom view.

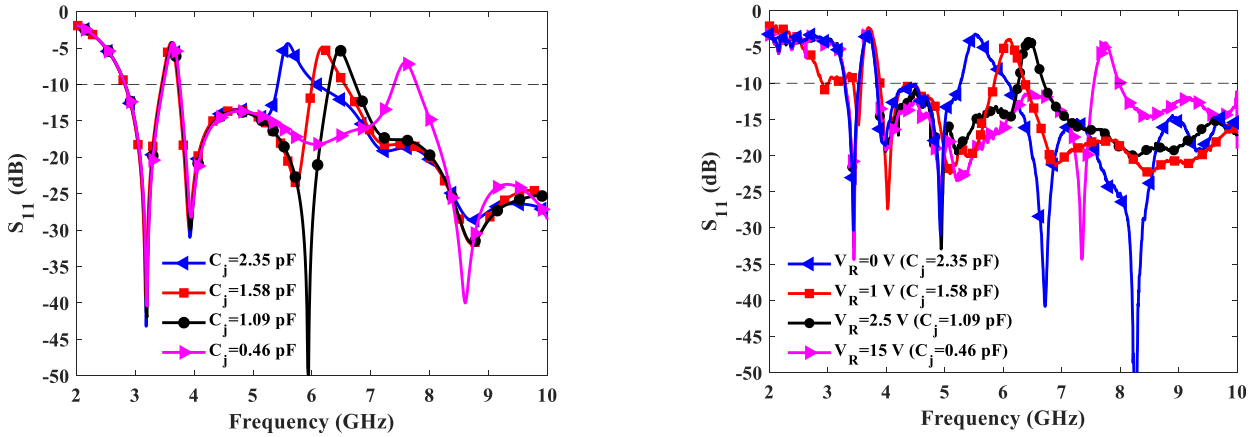

(a) (b)

Figure 10. Reflection coefficient spectrum of the designed dual notch band UWB antenna: (a) simulated results for different values of junction capacitances C_j and (b) measured results for relevant values of reverse bias voltages V_R.

3. RESULTS AND DISCUSSION

The designed dual notch band UWB antenna is fabricated and measured to demonstrate the tunability operation of the band notches experimentally. Fig. 9 shows photographs of the manufactured antenna from the top and bottom viewpoints. To keep the DC bias voltage isolated from the RF signal, a pair of 680 kΩ resistors are inserted into the structure. The simulated and measured reflection coefficient (S_{11}) results for different values of the junction capacitance C_j (experimentally the reverse bias voltage V_R) are presented and compared in Fig. 10. The first notch band occurs at the center frequency of 3.6 GHz, which can be tuned by changing the length of the semi-elliptical slot L_{s1} as investigated in Section 2.2. When the value of the reverse bias voltage V_R is increased from 0 V to 15 V, the center frequency of the second notch band can be tuned throughout a wide range from 5.6 GHz to 7.7 GHz, avoiding electromagnetic interference with upper WLAN and X-band systems. The performance of the designed antenna shows a good impedance matching over the UWB spectrum that further confirms the applicability of this antenna. It can be seen from Fig. 10 that simulated results are in good agreement with measured ones.

The case $V_R = 1$ V ($C_j = 1.58$ pF) is arbitrarily selected to investigate the simulated and measured radiation characteristics. The realized gain of the designed dual notch band UWB antenna is simulated and measured at this reverse bias voltage. Both simulated and measured gains drop dramatically at the

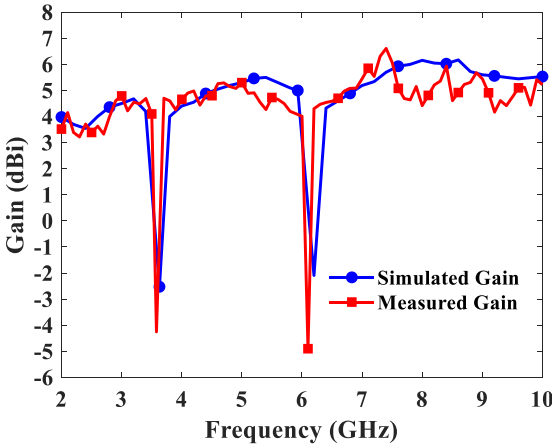

Figure 11. Simulated and measured realized gain of the designed dual notch band UWB antenna as a function of frequency.

two notch band frequencies around 3.6 GHz and 6.2 GHz, as seen in Fig. 11, while it is between 4 and 6 dBi in the UWB frequency region. A comparison between simulated and measured radiation patterns of the designed UWB antenna in E- and H-planes (principle planes) at 3.8 GHz, 6.5 GHz, and 8.7 GHz is presented in Fig. 12. Because this is a monopole UWB antenna, an omnidirectional radiation pattern is expected. Fig. 12 shows that the designed antenna, as a common monopole antenna, has steady radiation specifications in the E-plane and H-plane, with bidirectional and omnidirectional radiation patterns, respectively. In the E-plane, the radiation patterns resemble a figure of eight, whereas in the H-plane, the patterns are almost omnidirectional.

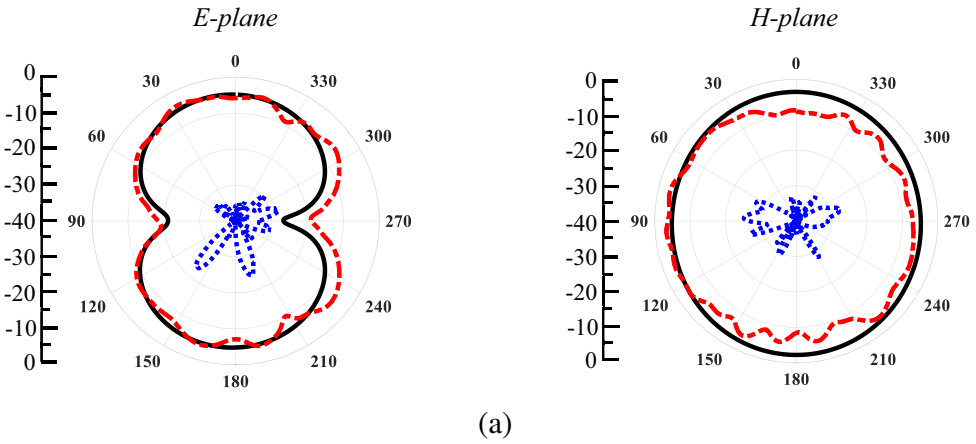

(a)

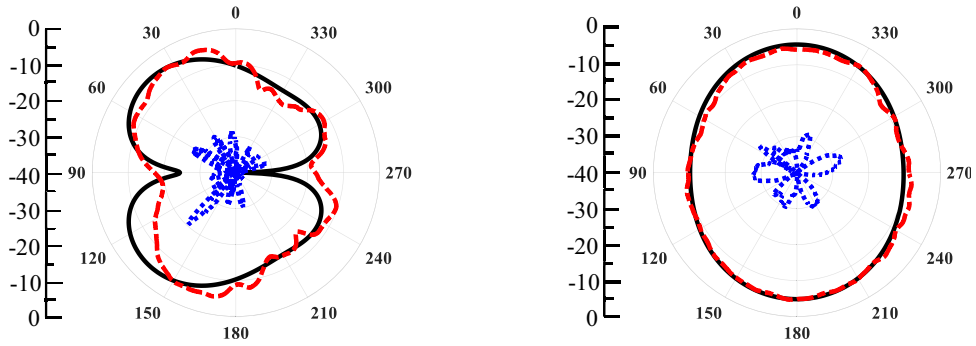

(b)

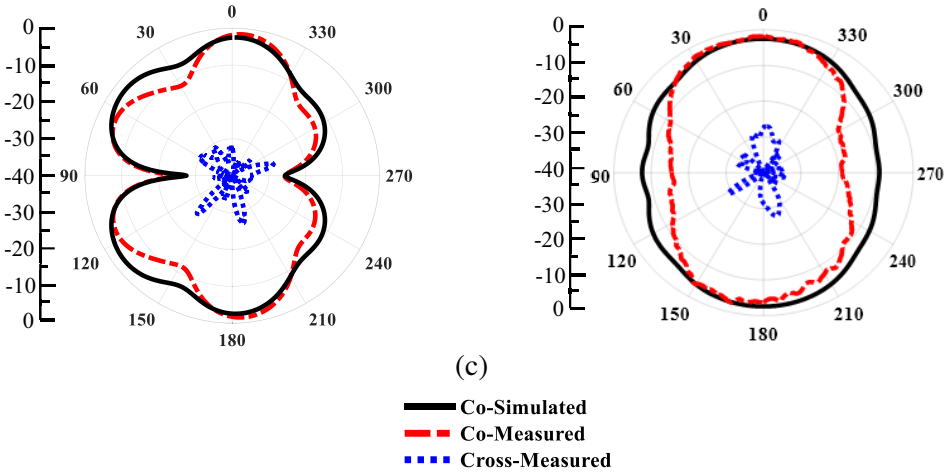

Figure 12. The comparison between simulated and measured radiation patterns, E-plane (left column) and H-plane (right column), of the designed monopole UWB antenna at three frequencies: (a) 3.4 GHz, (b) 6.2 GHz, and (c) 8.7 GHz.

Table 3. Comparison of the designed dual notch band antenna with existing prototypes.

Ref	Dimension of antenna (mm × mm)	Bandwidth (GHz)	Notch generation technique	Peak gain (dBi)	No. of notches	Tunable method used	Tuning range (GHz)
[15]	49.4 × 35	3.1–10.6	S-SRR-loaded feed line	6	1	Varactor	3.1–5.6
[16]	25 × 30	3.1–10.6	Open ended stubs	5	3	Varactor	3.31–3.57, 5.26–5.45, 5.78–5.91
[17]	31.3 × 34.9	1.98–10.54	CSRR slots	4	3	Varactor	1.58–2.12, 2.24–2.68, 3.08–3.78
[20]	30 × 31	3.1–10.6	Open ended loaded resonators	5	2	Capacitor	3–4, 5–6
[21]	32 × 32	3.1–19.3	Open loop resonators	4	1	Capacitor	5.1–6.5
[22]	24 × 24	Not mentioned	EBG structures	4	2	Varactor	2.80–4.00, 4.70–6.20
[23]	30 × 36	2.6–14	Inverted U-shaped slots	5	2	Varactor	5.58–5.91, 7.02–7.45
This work	26 × 36.6	3.1–12.5	Semi-elliptical and annular slots	6	2	Varactor	5.6–7.7

A comparison between the designed dual notch band UWB antenna and other UWB antennas is shown in Table 3. To conclude, the designed antenna has a well-set size, considerable gain, and a large tuning range. This study's unique feature is the creation of two rejection bands by using two slots on the patch while one notch band frequency is fixed in WiMAX, and the other is continuously tunable in a wide range from upper WLAN to X-band.

4. CONCLUSION

A compact monopole UWB antenna with dual notch band features on a $36.6 \times 26 \times 1\,\text{mm}^3$ low-cost FR-4 substrate has been presented for UWB applications. Two rejection bands have been designed by inserting a semi-ellipse slot and an annular slot centered at 3.6 GHz and 7.4 GHz on the radiating patch to avoid the interference of UWB systems with WiMAX, WLAN, and X-band devices. Simulation and measurement results agree well and validate the fabricated antenna for UWB systems operating in the frequency range 3.1–12.5 GHz with two notch band characteristics: the first is fixed at 3.6 GHz, and the

second is loaded with a varactor diode that allows it to be continuously tunable in the frequency range of 5.6 to 7.7 GHz. Moreover, compact size, significant gain, and omnidirectional patterns results have been achieved in the UWB frequency band.

REFERENCES

1. Immoreev, I. Y., "Practical applications of UWB technology," *IEEE Aerospace and Electronic Systems Magazine*, Vol. 25, 36–42, 2010.
2. Verbiest, J. R. and G. A. E. Vandenbosch, "Low-cost small-size tapered slot antenna for lower band UWB applications," *Electron Lett.*, Vol. 42, 670–671, 2006.
3. Zheng, Z. A. and Q. X. Chu, "CPW-fed ultra-wideband antenna with compact size," *Electron Lett.*, Vol. 45, 593–594, 2009.
4. First report and order on ultra-wideband technology, FCC, Washington, DC, USA, 2002.
5. Garg, R. K., M. V. D. Nair, S. Singhal, and R. Tomar, "A new type of compact ultra-wideband planar fractal antenna with WLAN band rejection," *Microwave Opt. Technol. Lett.*, Vol. 62, 2537–2545, 2020.
6. Kumar, G., D. Singh, and R. Kumar, "A planar CPW fed UWB antenna with dual rectangular notch band characteristics incorporating U-slot, SRRs, and EBGs," *Int. J. RF Microw. Comput. Aided Eng.*, Vol. 31, 22676(1–16), 2021.
7. Rehman, S. U. and M. A. S. Alkanhal, "Design and system characterization of ultrawideband antennas with multiple band rejection," *IEEE Access*, Vol. 5, 17988–17996, 2017.
8. Jeong, M. J., N. Hussain, H. Bong, J. W. Park, K. S. Shin, S. W. Lee, S. Y. Rhee, and N. Kim, "Ultrawideband microstrip patch antenna with quadruple band notch characteristic using negative permittivity unit cells," *Microwave Opt. Technol. Lett.*, Vol. 62, 816–824, 2019.
9. Mewaraa, H. S., J. K. Deegwalb, and M. M. Sharma, "A slot resonators based quintuple band-notched Y-shaped planar monopole ultra-wideband antenna," *AEUE-Int. J. Electron Commun.*, Vol. 83, 470–478, 2018.
10. Luo, S., Y. Chen, D. Wang, Y. Liao, and Y. Li, "A monopole UWB antenna with sextuple band-notched based on SRRs and U-shaped parasitic strips," *AEUE-Int. J. Electron Commun.*, Vol. 120, 153206(1–9), 2020.
11. Alhegazi, A., Z. Zakaria, N. A. Shairi, M. I. Ibrahim, and S. Ahmed, "A novel reconfigurable UWB filtering-antenna with dual sharp band notches using double split ring resonators," *Progress In Electromagnetics Research C*, Vol. 79, 185–198, 2017.
12. Orugu, R. and N. Moses, "Triangular fractal loaded reconfigurable antenna with notch band characteristics," *International Journal of Numerical Modeling Electronic Networks, Devices and Fields*, Vol. 34, 2806(1–11), 2020.
13. Nejati Jahromi, M., M. Nagshvarian Jahromi, and M. U. Rahman, "A new compact planar antenna for switching between UWB, narrow bandand UWB with tunable-notch behaviors for UWB and WLAN applications," *ACES Journal*, Vol. 33, 400–406, 2018.
14. Tang, M., H. Wang, T. Deng, and R. W. Ziolkowski, "Compact planar ultrawideband antennas with continuously tunable, independent band-notched filters," *IEEE Trans. Antennas Propag.*, Vol.64, 3292–3301, 2016.
15. Horestani, A. K., Z. Shaterian, J. Naqui, F. Martin, and C. Fumeaux, "Reconfigurable and tunable S-shaped split ring resonators and application in band-notched UWB antennas," *IEEE Trans. Antennas Propag.*, Vol. 64, 3766–3776, 2016.
16. Kingsly, S., D. Thangarasu, M. Kanagasabai, M. G. N. Alsath, S. K. Palaniswamy, T. R. Rao, S. Subbaraj, Y. P. Selvam, P. Sambandam, and G. Ganesan, "Tunable band notched high selective UWB filtering monopole antenna," *IEEE Trans. Antennas Propag.*, Vol. 67, 5658–5661, 2019.
17. Shome, P. P., T. Khan, and R. H. Laskar, "CSRR-loaded UWB monopole antenna with electronically tunable triple band-notch characteristics for cognitive radio applications," *Microwave Opt. Technol. Lett.*, Vol. 62, 2919–2929, 2020.

18. CST Microwave Studio 2019, CST Gmbh (http://www.cst.com) (2019).
19. Skyworks Data Sheet, Skyworks Solutions, Inc., Available at www.skyworksinc.com.
20. Xi, L., H. Zhai, Y. Zang, and L. Li, "A novel dual-band tunable band-notched antenna," *Microwave Opt. Technol. Lett.*, Vol. 59, 3014–3018, 2017.
21. Ali, W. A. E. and A. A. Ibrahim, "Tunable band-notched UWB antenna from WLAN to WiMAX with openloop resonators using lumped capacitors," *ACES Journal*, Vol. 33, 603–609, 2018.
22. Trimukhe, M. A. and B. G. Hogade, "Compact UWB antenna with tunable band-notch characteristics using varactor diode," *Progress In Electromagnetics Research C*, Vol. 97, 15–28, 2019.
23. Rai, V. K. and M. Kumar, "Tunable inverted U-shaped dual band notch monopole antenna for ultrawideband applications," *IETE Journal of Research*, 2021.